International Journal of Applied Engineering Research ISSN 0973-4562 Volume 14, Number 10 (2019) pp. 2388-2398


# High Empirical Study of IRIS Region Recognition Using RED Algorithm Based Discrete wavelet Transform

**Ala'a K. Al-Azzawi [1]**

*[1]Ministry of Higher Education & Scientific Research, Middle Technical University, Technical Engineering College, Department of Mechatronics Engineering, Baghdad-Iraq.*

**Abstract**

In this paper, a biometric recognition system based on the iris of a human eye using discrete wavelet transform (DWT) and multi support vector machine classifier is proposed. The classifier is used to classify the iris zoom into three categories: cut transition, gradual transition and normal sequences. A compact low pass filter with an exponential weighted moving average in a RED algorithm is extensively used. The algorithm can be used to calculate the average queue size as well as maintain high throughput and low delay. Before extracting the features of an iris, the input image is pre-processed to localize, segment and enhance the region of interest, blurring, and artifacts especially those associated with edges. The block textural information of a person's iris is exploited to categorize the input image into a number of vectors (blocks). The categorizing of these blocks were based on extracting the edge in different direction from wavelet transition coefficients in a given image block. Furthermore, computing of block variance and directional variances of neighboring blocks greatly facilitated the reconstructing of the strong diagonal edges. Best extraction of vertical, horizontal, and diagonal image gradients were computed. The largest numbers of these gradients were obtained after changing both the magnitude of the threshold, which were extracted from histograms of those gradients, and the boundary match vector angles. Experimental results show that the proposed method is quite fast efficient and accurate method employs a minimum distance classifier according to hamming distance.

**Keywords:** Region recognition; discrete wavelet transform (DWT); Block textural; Random Early Detection (RED) algorithm; feature selection.

## 1. INTRODUCTION

Biometric based person identification is getting popular due to its accuracy and high reliability. In iris recognition biometric, iris is believed to be more artless as it can't be artificially copied and also it remains same during a person's life time. Iris recognition is the process of recognizing a person by analyzing the random pattern of the iris [1]. Before recognition of the iris takes place, the iris is located using preeminent features. These preeminent features and the differentiated shape of the iris allow for imaging, feature isolation, and extraction [2]. Localization of the iris is an important step in iris recognition because, if done improperly, resultant noise (e.g., eyelashes, reflections, pupils, and eyelids) in the image may lead to poor performance.

Iris imaging requires use of a high quality digital camera. By making use of imaging an iris, a 2D Gabor wavelet filters and maps the segments of the iris into vectors. These vectors include information on the orientation and spatial frequency and the position of these areas. This seems to be the optimal basis to extract local features and map the Iris codes. Iris patterns are described by an iris code using phase information collected in the vectors.

The two iris code templates are compared by computing the hamming distance between them. The hamming distance is a fractional measure of the number of bits disagreeing between two binary patterns. Hamming distance approach is a matching employed by daugman for comparing two bit patterns and it represents the number of bits that are different in the two patterns.

Extracting of iris image data is the major iris recognition standards. The segmentation localizes the iris's spatial extent in the eye image by isolating it from other structures in its vicinity, such as the sclera, pupil, eyelids, and eyelashes. Image segmentation is typically used to locate objects and boundaries (lines, curves, etc.) in images. Further, to define two data formats for representing an iris image. The first format utilizes a rectilinear format in which the image can be raw or compressed and can vary in size based on field of view and compression or color (gray or color intensity levels). The second format utilizes a polar image specification with specific preprocessing and segmentation steps for the image, which can be raw or compressed; contains only iris information.

The algorithms used in an iris-recognition first have to localize the inner and outer boundaries of the iris (pupil and sclera) in an image of an eye. Further subroutines detect and exclude eyelids, eyelashes, and specular reflections that often occlude parts of the iris. Among all the biometric techniques iris recognition has drawn a lot of interest in Pattern Recognition and Machine Learning research. As it is more unique, stable, universal and do not depend upon genetics [3], [4].

The iris verification can be divided into five stages: (i) Data Acquisition module, (ii) Preprocessing module (includes segmentation) (iii) The normalization module invokes a geometric normalization scheme to transform the segmented iris image from Cartesian coordinates to polar coordinates. (iv)The encoding module uses a feature-extraction routine to produce a binary code. And (v) The matching module determines how closely the produced code matches the

encoded features stored in the database [5], [6], [7]. A good biometric is characterized by the use of a feature that is; highly unique – so that the chance of any two people having the same characteristic will be minimal, stable – so that the feature does not change over time, and be easily captured – in order to provide convenience to the user, and prevent misrepresentation of the feature. The rest of the paper is organized as follows. In section 2, the definition of a RED algorithm and its analysis are introduced, and important mathematical properties are included. Section 3 presents the theory of the iris recognition system, followed by wavelet based energy features. The methodology and a preprocessing classification on iris image followed by the proposed method are presented in section 4. Experimental results and discussions are depicted in Section 5. Finally, section 6 concludes the presented work.

## 2. RANDOM EARLY DETECTION (RED) ALGORITHM

RED algorithm was first proposed by Sally Floyd and Van Jacobson in [8], for active queue management (AQM) and then standardized as a recommendation from IETF in [9]. As such, RED is able to avoid global synchronization of TCP flows, maintain high throughput as well as a low delay and achieves fairness over multiple TCP connections, etc. The RED algorithm calculates the average queue size $\boldsymbol{Q_S}$ using a low pass filter with an exponential weighted moving average. The average queue size is compared to two thresholds: $\boldsymbol{TH_{min}}$ **and** $\boldsymbol{TH_{max}}$.

**When:**

- $\boldsymbol{Q_S} < \boldsymbol{TH_{min}}$, no packets are marked.
- $\boldsymbol{Q_S} > \boldsymbol{TH_{max}}$, every arriving packet is marked.
- $\boldsymbol{TH_{min}} \overset{Q_S}{\Leftrightarrow} \boldsymbol{TH_{max}}$, each arriving packet is marked with probability $\boldsymbol{P_{ave}}$, where $\boldsymbol{P_{ave}}$ is a function of the average queue size.
- $\boldsymbol{Q_S} -=$ Does not significantly exceed $\boldsymbol{TH_{max}}$, if marked packets are, in fact, dropped or if all source nodes are cooperative.

Substantially, RED algorithm has two separate parts. One is for calculating the $\boldsymbol{Q_S}$, which determines the degree of burstiness that will be allowed in the router queue. It takes into account the period when the queue is empty (the idle period) by guessing the number $m$ of small packets that could have been transmitted by the router during the idle period. Seamlessly, the router computes the average queue size as if $m$ packets had arrived to an empty queue during that period.

The optimal value of the packet-marking probability is calculated by the second part to determine how frequently the router marks packets, given the current level of congestion. Hence, the optimal value of the marking probability is derived to then present a new marking scheme to fully exploit its benefits as well as to reduce the total number of packets needed by the victim to reconstruct the attack path [10]. The goal is for the router to mark packets at fairly evenly spaced intervals, in order to avoid biases and avoid global synchronization, and to mark packets sufficiently frequently to control the average queue size.

## 3. THEORY OF IRIS RECOGNITION SYSTEM

Iris recognition is the process of recognizing a person by analyzing the random pattern of the iris (Figure 1) [11].

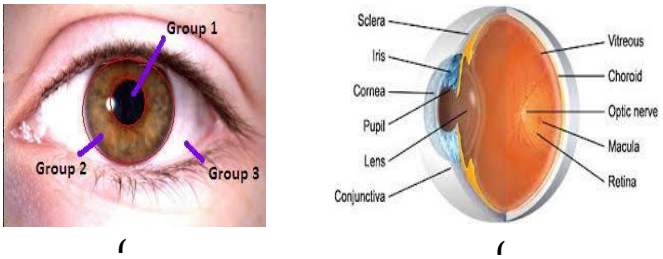


**Fig. 1** Human eye; (a) eye groups, (b) iris sample

The iris is a muscle within the eye that regulates the size of the pupil, controlling the amount of light that enters the eye. It is the coloured segment of the eye with colouring based on the density of melanin tincture within the muscle (Figure 2). Iris recognition technology combines computer vision, pattern recognition, statistical inference, and optics.

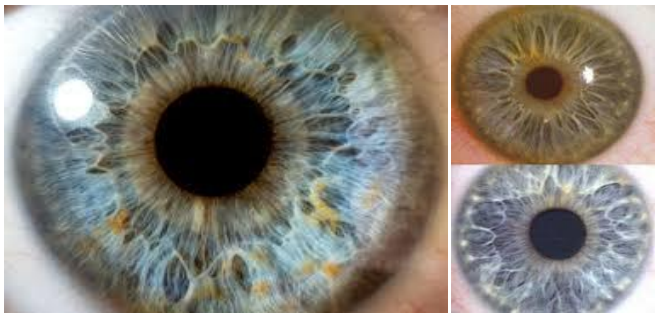

**Fig. 2** Colored portion of eye

Algorithms described in [12] for encoding and recognizing iris patterns have been the executable software used in all iris recognition systems so far deployed commercially or in tests. There exist many alternative methods for finding and tracking facial features such as the eyes. The input to the system will be an eye image, and the output will be an iris template, which will provide a mathematical representation of the iris region. In these trials, most imaging was done without active pan/tilt camera optics, but instead exploited visual feedback via a mirror or video image to enable cooperating.

### 3. 1 Wavelet Based Energy Features

In wavelet transform (WT), the image is represented in terms of frequency content of local regions over a range of scales. DWT decompose an image into four sub-bands, which is the low frequency LL, the vertical high frequency LH, the horizontal high frequency HL, and the diagonal high frequency HH respectively. The low frequency looks very similar to the original image but the size is a half of the

original one through a down sampling. The LH includes the information about a vertical element of the original image, which depicts the vertical directional edge of the original image. Similarly, the HL is the horizontal directional edge of the original image. The HH corresponds to the diagonal directional edge of the original image. In this case, large color and edge features can be captured from the DWT image [13]. Therefore, data is initially subjected to standard histogram equalization to adjust the intensity of images. To represent an image into several sub images and analyzes them in the frequency domain multi resolution analysis is used. Then the discrete wavelet transform (DWT) features are extracted and pre-processed. Then the features are normalized using z-score normalization technique. These features are then ranked using chi squared, gain ratio, information gain feature evaluation techniques and relief feature ranking schemes. The features are selected using for consistency subset evaluation strategies: best first, random search, genetic search and greedy search. The following Fig. 3 shows the low frequency LL "haar" decomposition iris image.

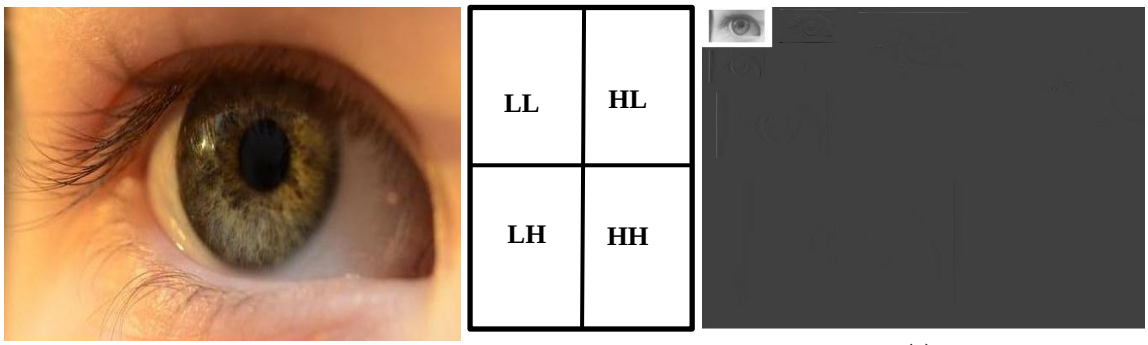


(a) (b) (c)

**Fig. 3** Discrete wavelet transform (DWT); (a) iris image to be decomposed, (b) decomposing of wavelet transform into four sub-bands iris images, (c) low frequency (LL) wavelet transform iris image.

## 4. METHODOLOGY

The first step of this work is devoted to capture large color and edge features of different color iris images. In this context, various preprocessing steps are carried out. It includes a successive conversion of color image to gray scale, histogram equalization, circle extraction, and segmentation. The color and the edge in the vertical, the horizontal and the diagonal direction are chose as the features vector.

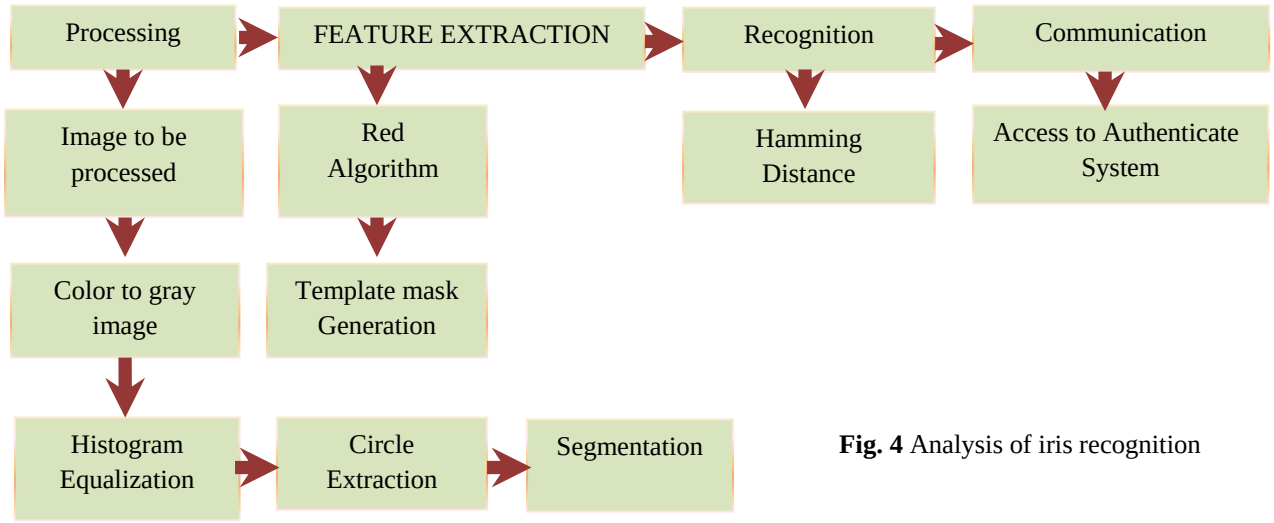


**Fig. 4** Analysis of iris recognition

The generation of template is elicited after applying polar to rectangular conversion and on this rectangular template RED algorithm is applied. These templates are match with the stored one using hamming distance and the match ID is displayed. Figure 4 shows the flow of the process.

### 4.1 Preprocessing

#### 4.1.1 DWT Based Feature Extraction

Image feature extraction is very important in image processing technique to detect and isolate desired portions of an image. After extraction of the meaningful coefficients from the region of interest (ROI's), 3-level "haar" decomposition

DWT is applied for extracting coefficients to obtain the texture information. In other words, DWT is a technique used to extract features from a given images, which extracts maximum highlighting pixels present in images to progress results. In this context, 3 step procedures for automatic detection of meaningful image features is used. The steps are preprocessing, feature extraction and classification [14-15].

The variation of the extracted color features between multiple iris images can be calculated according to LL bands of each decomposed image. The difference of the edge in the vertical, the horizontal and the diagonal direction of multiple iris images can be computed depending on the HL, LH, and HH bands of each decomposed iris image respectively.

***1) Color Difference***

Let $T(I)$ denote the total of the low frequency coefficient $(LL)$ of the iris image $(I)$, which can be computed by the following formula.

$$T(I) = \sum_{k=1}^{N_T} Coeff\,(k) \quad (1)$$

Where $Coeff(k)$ is the coefficient value, $N_T$ represents the total number of the low frequency coefficient of the iris image.

The color difference between two iris images can be calculated by the following formula.

$$C_t(I) = T_t(I) - T_{t+1}(I) \quad (2)$$

Where $C_t(I)$ is the color difference of one block between two iris images?

In order to omits smooth intervals, produce a new sequence named $C_t'(I)$ according to the following formula.

$$C_t'(I)\ \{\begin{matrix} 0 & C_t(I) < T_D \\ 1 & otherwise \end{matrix} \quad (3)$$

Finally the difference between two iris images based on their color feature is given from the following equation:

$$T_D^{LL} = \sum_{I=1}^{N_T} C_t'\,(I) \quad (4)$$

In which, $N_T$ represents the total number of block of iris image.

***2) Edge Deference***

Similarly, applying the same procedure of the above color difference algorithm. The difference between two images based on their edge feature in the vertical, the horizontal and the diagonal direction can be estimated after applying the above four equations (1) – (4), which denote by $T_D^{HL}, T_D^{LH}, and\ T_D^{HH}$ respectively.

### 4.1.2 Histogram Equalization

Histogram equalization is a technique for adjusting image intensities to enhance contrast. The levels of a gray shadow images are considered as a random variables in the interval [0 1], in which the random variables were usually attributed to the probability density function. In this context, the average length of information to be encoded and assigned by the values of various gray levels can be calculated by summing the product of the number of bits used to represent each gray level and probability of occurrence of gray level.

Let $I$ be a given image represented as a $X_R$ by $X_C$ matrix of integer pixel intensities ranging from 0 to L − 1. L is the number of possible intensity values, often 256. Let $H$ denote the normalized histogram of $I$with a bin for each possible intensity. So

$$H_n = \frac{number\ of\ pixels\ with\ intensity\ n}{total\ number\ of\ pixels} \qquad n = 0, 1, \ldots\ldots\ldots L-1 \quad (5)$$

The histogram equalized image $I_E$ will be defined by

$$I_{E\,i,j} = floor((L-1)\sum_{n=0}^{I_{i,j}} H_n)) \quad (6)$$

Where floor() rounds down to the nearest integer. This is equivalent to transforming the pixel intensities, k, of $I$ by the function

$$T_k = floor(L-1)\ \sum_{n=0}^{k} H_n \quad (7)$$

The motivation for this transformation comes from thinking of the intensities of $I$ and $I_E$ as continuous random variables X, Y on [0, L − 1] with Y defined by

$$Y = T(X) = (L-1)\int_0^x px\,(x)dx \quad (8)$$

Where $px$ is the probability density function of $I$. $T$ is the cumulative distributive function of X multiplied by (L − 1). Assume for simplicity that $T$ is differentiable and invertible. It can then be shown that Y defined by $T(X)$ is uniformly distributed on [0, L −1], namely that $p_Y(y) = \frac{1}{L-1}$.

### 4.1.3 Image Segmentation

Image segmentation is a process in which regions or features sharing similar characteristics are identified and grouped together. The assertive aim in image processing applications is to extract important attributes from the iris image data, from which an interpretative prospect can be achieved by the machine. Most of images have been appropriately preprocessed to eliminate noise and artifacts. Segmentation is often the key step in interpreting the image. Many statistical techniques are used to either accurately delineate the boundary separating of distinct regions or to group these regions according to their anatomical or functional roles [16]. In this work, both artificial neural network and nearest-neighbor classifier methods have been used for image segmentation. The output of the segmentation step is usually a set of classified elements used to get an initial estimate of the region. As a result, this leads to achieve more accurate representation of the target boundary, in which each pixel classified in the same class as the training actuality with the closet intensity [17-18].

The basic purpose of region growing is to segment an entire image $F$ into smaller sub-images, $F_i$, $i = 1, 2, \ldots, N$. Which satisfy the following conditions [18]?

$$F = \cup_{i=1}^{N} F_i\ ;\ F_1 \cap F_j = \Phi, i \neq j \quad (9)$$
$$H(F_i) = True; i = 1, 2, \ldots, N;$$

When $F_i$ and $F_j$ are adjacent:

$$H(F_i \cup F_j) = False, i \neq j;$$

The left and right boundaries of the iris are found by selecting the largest gradient change to the left and right of the pupil. The iris segmentation approach is based on the fact that the

pupil is typically darker than the iris and the iris is darker than the sclera [2]. As shown in Fig. 5, the region represents the pupil-iris and iris-sclera gradient change.

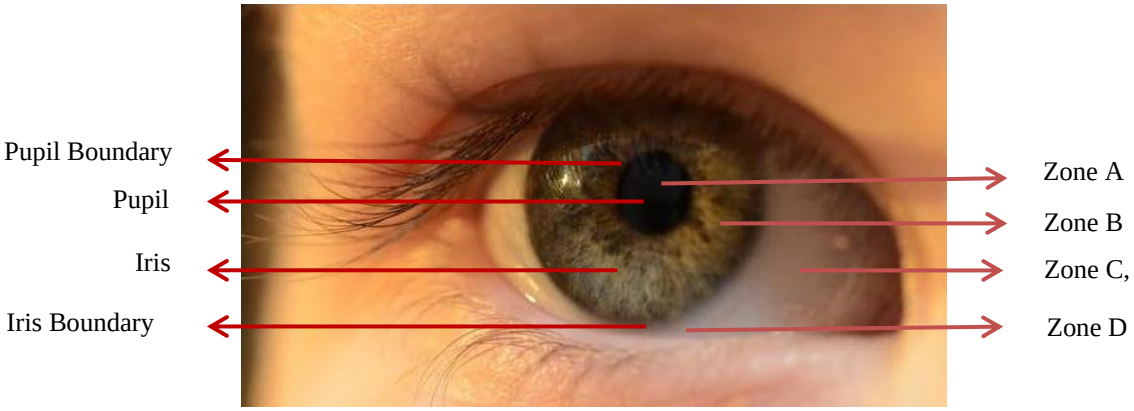


**Fig. 5:** Is the original image with the projected right region: zone A represents pupil area with a dramatic change of pupil iris gradient; zone B represents the clearer pixels in the iris pattern; zone C represents the gradient change between iris and sclera followed by much whiter pixels of the sclera in zone D.

Figure 6 shows both an ideal example of image segmentation and the over-segmentation flow chart used to eliminate boundaries that are not in edge detection result. In order to accomplish the edge detector algorithm, successive steps must be followed. The first step is to compress and filtering out the original image to tackle the problems of invisible patches, blockiness, blurring, and artifacts effects located at the boundaries. The essential goal behind block-based compression is to interpolate the DCT coefficients of missing blocks from those with the same position in the neighboring blocks. In other words, the idea behind a block-based compression is the ease of dealing with the blocking artifacts located at the block boundaries of sub bands, as well as tackling these artifacts.

Therefore, the energy distribution in the DCT domain determines the edge patterns in the spatial block. Hence, the lost pixels are interpolated by a linear combination of coefficients in the DCT domain.

Three measures of different edge patterns, the horizontal edge $H_{Edge}$, the vertical edge $V_{Edge}$, and the diagonal edge $D_{Edge}$ are calculated from the DCT coefficients of the sub-block, to indicate whether has strong edge or not.

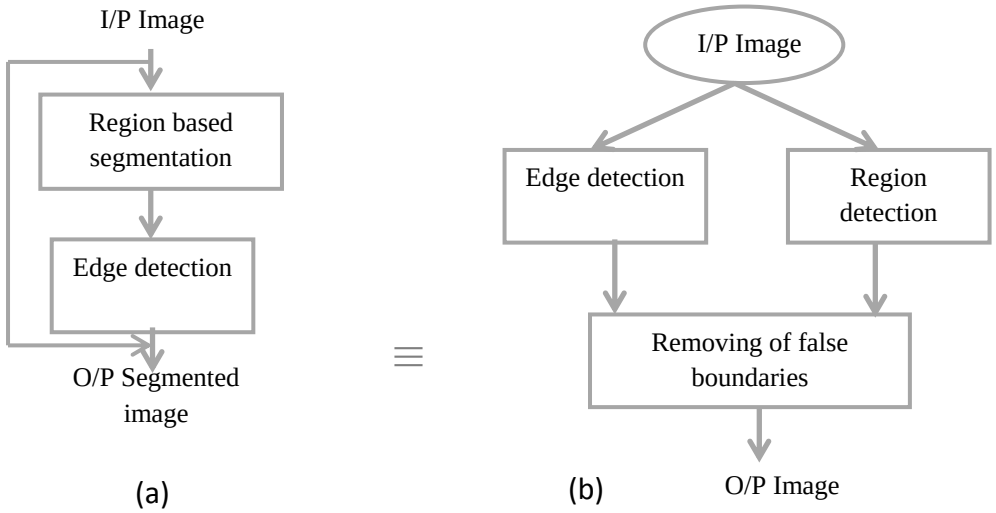


**Fig 6:** (a) An ideal example of image segmentation. (b) Flow-chart for image segmentation combining region and boundary information.

### 4.2 Proposed method

The following Fig. 7 shows the proposed segmentation flow chart used for extracting the meaningful features of selected blocks in a multiple iris images. The goal of this process is to satisfy the segmented parts first the non-specific parts are removed that are not parts of the interested region. A classifier called support vector machine (SVM) has been used in order to classify the dimension of 3-dimensional volume that is parallel to a pixel as well as to obtain better results. The feature SVM has been constructed which is based on the coefficients of the DWT. The accuracies and the performance are provided in terms of training performance and the classification accuracies.

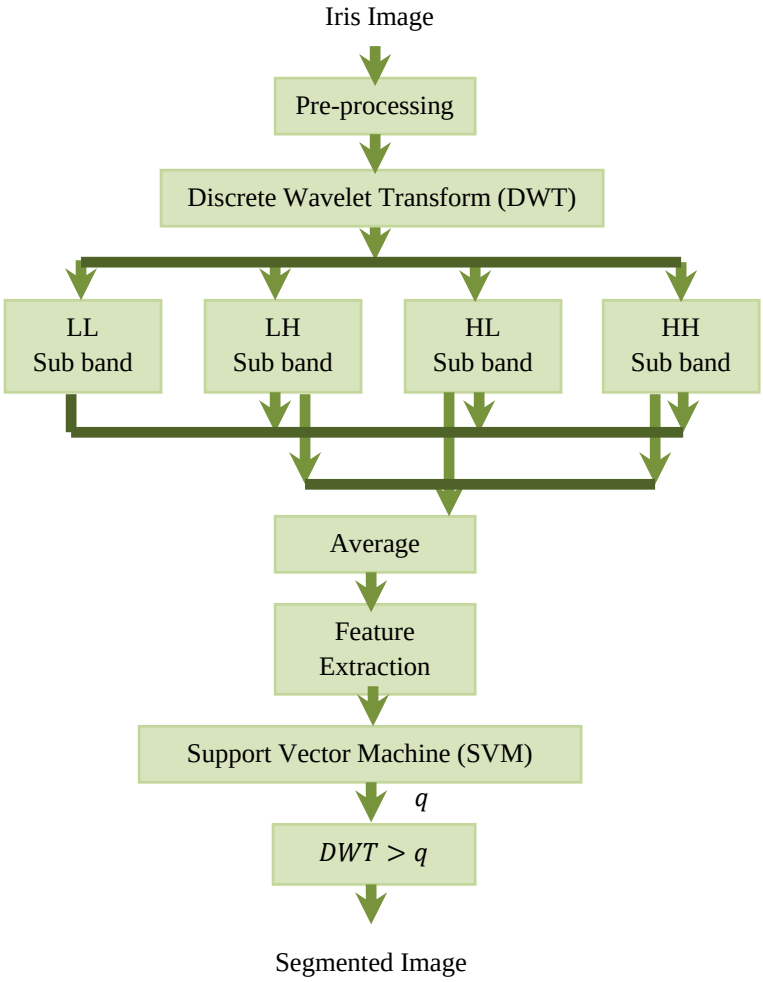


**Fig. 7** Proposed method flow-chart

In summary, the method can work when the block contains an edge that is not vertical or horizontal after the adoption of the DCT coefficients of the sub-block. Equation 10 has been used to decide whether the sub-block contains horizontal, vertical or diagonal edges.

$$\theta = \tan^{-1}\frac{Vertical\ \ edge}{Horizontal\ \ edge} = \tan^{-1}\frac{V_E}{H_E}, \quad \theta = 0^\circ \Rightarrow 90^\circ \quad \text{.....} \quad (10)$$

Where a $0^\circ$ degree means a horizontal edge, $90^\circ$ means a vertical edge, and $45^\circ$ is a diagonal edge.

## 5. EXPERIMENTAL RESULTS AND DISCUSSIONS

The following images show the experimental results of the iris which were implemented using MATLAB 2013a version with 4GB RAM and i5 processor. Extracting the edges from digital images is one of the most important steps in image processing, analysis and pattern recognition systems, as well as providing an indication of the physical extent of the objects within the components of the image. Figure 8 shows the detection of the fourth quadrants of the iris image. In first step the original RGB image is converted into a gray-scale phase. The DWT decomposed the original spatial-domain signal into various decomposition levels. The decomposition levels comprise a number of sub-bands, in which each of them contains the coefficients of the vertical, the horizontal and the diagonal

images. Figure 9 shows the results of the second step in which pupil region is stated by 20-80 intensity value of gray level. In contrast, three levels of "haar" decomposition of a high resolution binary iris image($432 \times 752\ pixels$)is extracted after using a specific thresholding.

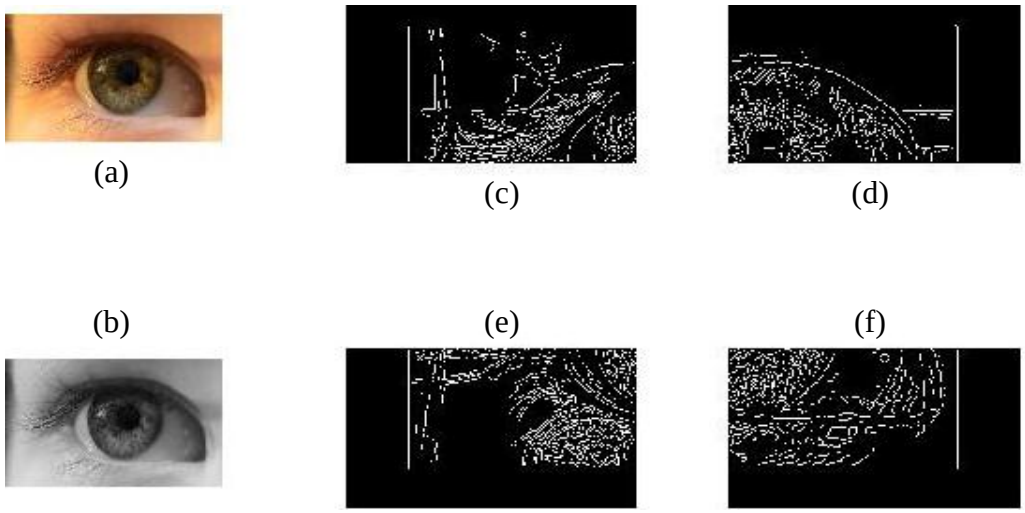


**Fig. 8** Iris edge detection using "Canny detector"; (a) original image, (b) gray-scale image, (c) first-quadrant edge detection, (d) second-quadrant edge detection, (e) Third-quadrant edge detection, (f) Fourth-quadrant edge detection.

To illustrate the idea of decomposition more accurately, figure 10 shows the result of eliciting the approximation of iris image as well as images of the sub-bands frequencies (vertical, horizontal, and diagonal images) of the three levels "haar" decomposition. Meanwhile, the figure shows the results of the third step after using the morphological operators opening and closing for removing some unwanted regions.

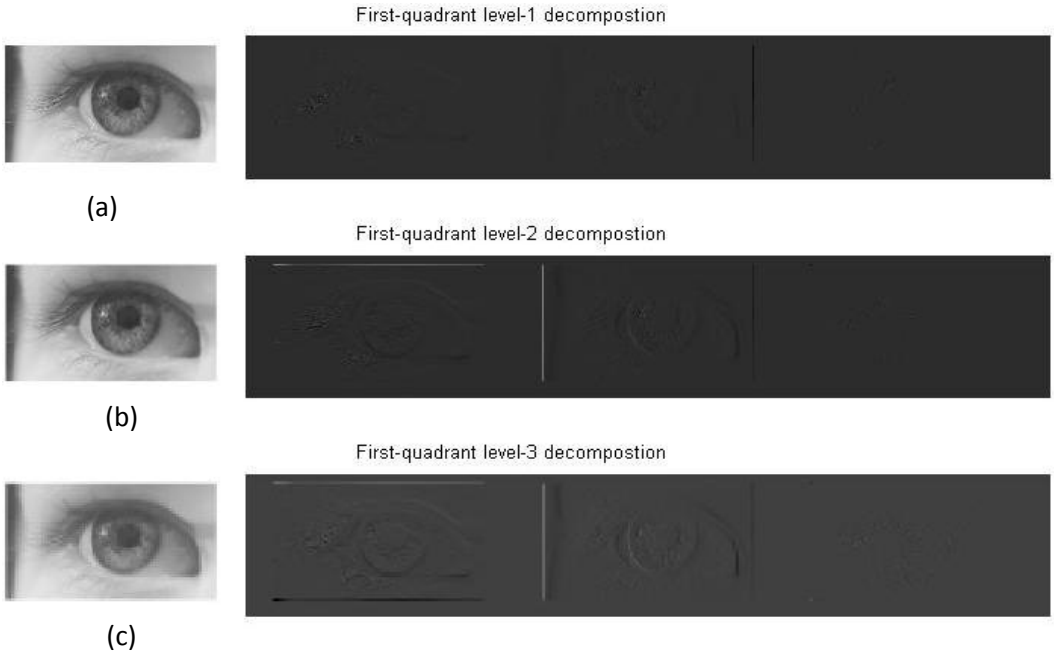


**Fig. 9** Binary iris image with 3-levels "haar" decomposition; (1) first-level decomposition, (b) second-level decomposition, (c) third-level decomposition.

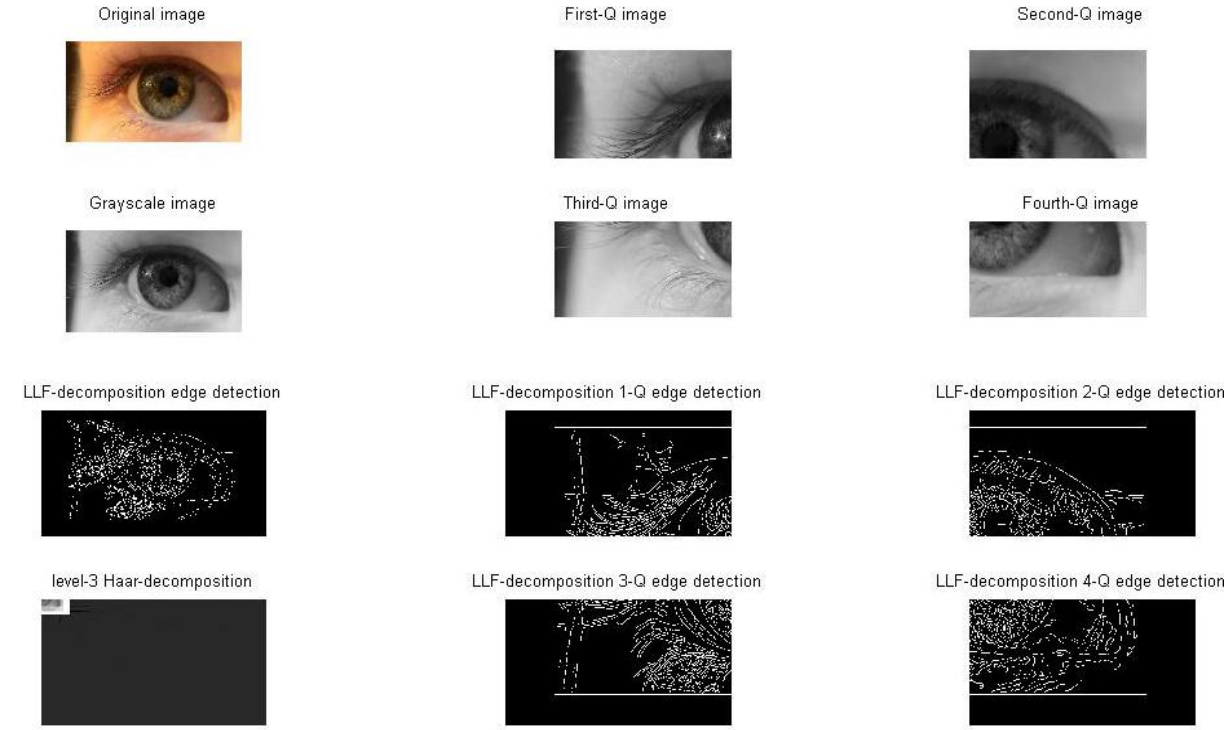


**Fig. 10** Low-Low-Frequency (LLF) resultant iris image edge detection after applying the morphological operator's with approximation "Haar" decomposition iris image.

The high-high, high-low, low-high, and low-low frequencies (HHF, HLF, LHF, and LLF) in the three levels of haar decomposition are shown in figure 11. Figure 11 shows the details and approximation of the iris image.

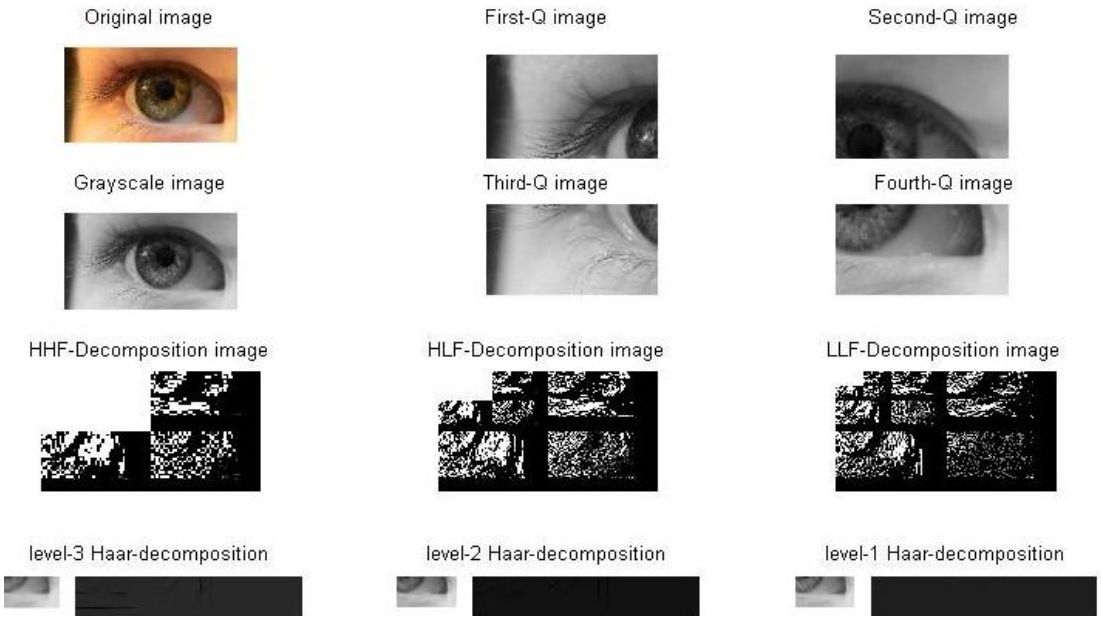


**Fig. 11** HH, HL, LH, and LL "haar" decomposition (details and approximation iris images)

The fourth step is devoted to distinguish between the eccentricities feature (pseudo) and benefits features hopefully to locate the true pupil region. As a result, eliciting the minimal unwanted features region considered as criterion to select the more significant values of area that is marked as pupil region. Fig. 12 shows the extracted pupil region.

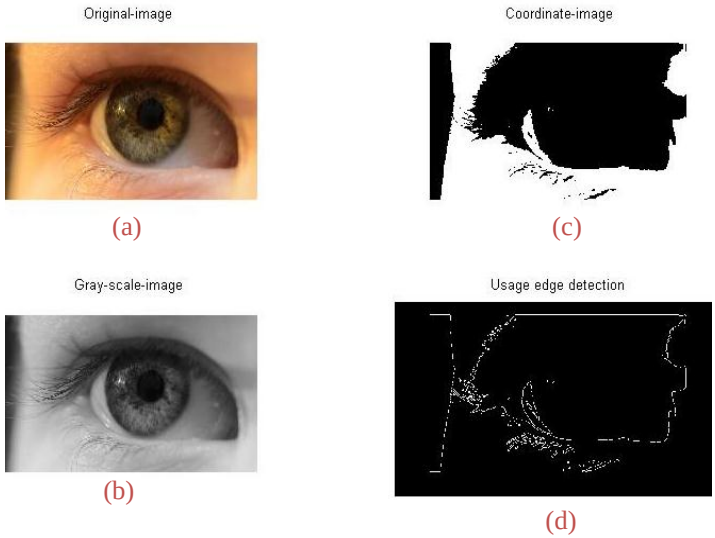


**Fig. 12** Minimal pseudo region; (a) original image, (b) gray-scale image, (c) coordinate-image, and (d) usage edge detection

The canny detector is a parallel differential operator used to extract edges of the images after evaluating the partial derivation in both $i$ and $j$ directions are evaluated after extracting the edges of images. They are predefined as $S_i$ and $S_j$ respectively.

The gradient of each pixel is evaluated using the following formula: $G(i,j) = \sqrt{(S_i^2 + S_j^2)}$. Further, a threshold magnitude $G_{TM}$ is evaluated for the purpose of comparison. If, $G(i,j) > G_{TM}$ this point is considered as an edge point. The partial derivatives in $i$ and $j$ directions. In other word, the direction of the edge is computed using the gradient in $i$ and $j$ directions and illustrated in eq. 11 and eq. 12.

$$S_i = \{F(i+1,\ j \pm 1) + 2F(i+1,j)\} - \{F(i-1,\ j \pm 1) + 2F(i-1,j)\} \quad (11)$$

$$S_j = \{F(i \pm 1,\ j+1) + 2F(i,j+1)\} - \{F(i \pm 1,\ j-1) + 2F(i,j-1)\} \quad (12)$$

The edge strength is assessed after the adoption of extracting both vertical and horizontal image gradients.

Accordingly, the gradients of the image are represented as follows:

$$\text{Im}age\ gradient = F_G(i,j) = \sqrt{V_G(i,j)^2 + H_G(i,j)^2} \quad (13)$$

Where, $V_G(i,j)$ and $H_G(i,j)$ are the vertical and horizontal image gradients, respectively, and calculated as follows:

$$V_G\ (\text{i, j}) = P(i,j) \otimes F_V(i,j) \quad (14)$$

$$H_G(i,j) = P(i,j) \otimes F_H(i,j) \quad (15)$$

The steps required for canny detector are as follows:

- **Smooth by Gaussian:**

First smooth the image by a Gaussian G! And then take derivatives: $\frac{\partial f}{\partial x} = \frac{\partial (G_\sigma * f)}{\partial_x}$. Applying the differentiation property of the convolution: $\frac{\partial f}{\partial x} = \frac{\partial\, G_\sigma}{\partial_x} * f$. Therefore, taking the derivative in x of the image can be done by convolution with the derivative of a Gaussian:

$$G_\sigma^x = \frac{\partial G_\sigma}{\partial_x} = x\, e^{-\frac{x^2+y^2}{2\sigma^2}} \quad (16)$$

For clarity, only the pixel with the largest gradient amplitude is the true edge. The detected edge pixel is calculated as:

$$\text{P}_{\text{Edge}} = \left\{(\text{V}_{\text{Edge}} * \text{k},\ \text{H}_{\text{Edge}} * \text{k}) \quad 1 \le \text{N},\ \text{k} \in \text{z}\right\} \quad (17)$$

Where, $N$ is denoted as the number of the detected edge pixels in the boundary pixels and surrounding the damaged block.

- **Compute gradient magnitude and orientation:**

Gradient magnitude and gradient orientation are expressed in terms of the two directional derivatives $\partial_{Vertical}(i,\ j)$ and $\partial_{Horizontal}(i,\ j)$ . Here, the gradient magnitude is defined as:

$$\left|\nabla F(i,j)\right| = \sqrt{(\partial_{Vertical}\ F(i,j))^2 + (\partial_{Horizontal}\ F(i,j))^2} \quad (18)$$

Where, $F(i,\ j)$ is a continuous image? $i$ and $j$are the row and column coordinates, respectively. The gradient orientation is given as:

$$\theta\ \ (i,j) = \tan^{-1}\frac{H_G(i,j)}{V_G(i,j)} \quad (19)$$

Table 1 shows the measuring of the mean square errors (MSE's) and the power signal-to-noise ratios (PSNR's) for both the vertical and the horizontal image gradients after changing the boundary match vector angles, and the magnitude of the threshold.

**Table 1** The calculating of MSE and PSNR for both vertical and horizontal image gradients

| **Theta** | $\theta = 0^{\circ}$ | | $\theta = +45^{\circ}$ | | $\theta = 135^{\circ}$ | |
|---|---|---|---|---|---|---|
| **Threshold** | 15% | 25% | 35% | 45% | 55% | 65% |
| **MSE-VG** | 0.0136 | 0.0028 | 0.0142 | 0.0043 | 0.0149 | 0.0036 |
| **MSE-HG** | 0.0114 | 0.0024 | 0.0118 | 0.0039 | 0.0123 | 0.0044 |
| **PSNR-VG** | 32.211 | 34.688 | 32.110 | 34.288 | 32.115 | 34.578 |
| **PSNR-HG** | 32.442 | 34.756 | 32.338 | 34.376 | 32.336 | 34.293 |

From the results shown in Table 1, it can be stated that as the magnitude of the threshold increased the measured of the MSE's for both the vertical and the horizontal image gradients will decrease. One can also observe that the measured of the PSNR's image gradients will increase. The simulated and measured results of the mean square errors (MSE) have been carried out in Fig. 13. These results illustrated the relationship between the vertical and the horizontal iris image gradients.

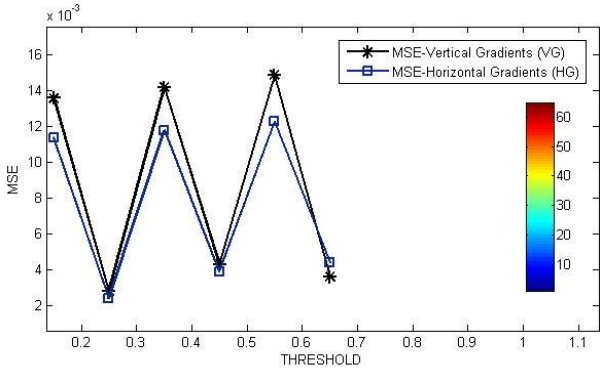


**Fig. 13** MSE's of the vertical and horizontal image gradients

## 6. CONCLUSION

In this paper, 2-D discrete wavelet transform (DWT) haar decomposition was presented. The empirical wavelet transform (EWT) is used to decompose the image into the lower resolution approximation image (LL) of the 2-level bi orthogonal discrete wavelet transform (DWT). Furthermore, usage features are obtained from decomposed EWT components. These features are used for the classification of normal images using least squares support vector machine classifier. The proposed technique used to have improved performance, specifically segment areas that contain edges with high accuracy. Next, high-quality image was properly guaranteed, after pre-processing the input image to localize the inner boundary and outer boundary of iris, segment and enhance the region of interest (i.e., iris zone). Thus resulting in a visually better iris image at the geometric information with minimal blurring and artifacts. Further, the block textural information was exploited to categorize the input data into a number of vectors (blocks). The categorizing of these blocks were based on the edge orientation in a given image block. For example, block variance and the directional variances of the four neighboring blocks. This greatly facilitated the reconstructing of the strong diagonal edges. The method provides very good extracting of strong edges. In this context, a best extraction for the vertical, horizontal and diagonal image gradients were achieved. The largest numbers of these gradients were obtained after changing both the magnitude of the threshold, which were extracted from histograms of those gradients, and the boundary match vector angles. The performance of the predicted images was also significantly improved, in terms of blurring and artifacts, especially those associated with edges. Further, a low pass filter with an exponential weighted moving average in a RED algorithm is used to calculate the average queue size as well as maintain high throughput and low delay.

**Acknowledgement**

I would like to thank all the staff of the department of electronics and communication engineering for their support and contribution through my research period. Also, I would like to thank my dean of the technical engineering college for offering an interesting paper topic and for his advice.

## REFERENCES

[1] Tariq M. Khan et al. "Automatic localization of pupil using eccentricity and iris using gradient based method" Optics And Lasers in Engineering, ELSEVIER, 49 (2011) 177-187.

[2] Sumeet Dua, Senior Member, IEEE, U. Rajendra Acharya, Pradeep Chowriappa, Member, IEEE, and S. Vinitha Sree, "Wavelet-Based Energy Features for Glaucomatous Image Classification", IEEE Transactions on Information Technology in Biomedicine, Vol. 16, No. 1, 2012.

[3] Y. Zhu, T. Tan, and P. Y. Wang, "Biometrics personal identification Based on Iris Patterns," 15th International Conference on Pattern Recognition, vol. 2, pp. 801-804, 2000.

[4] G. Annapoorani, R. Krishnamoorthi, P. G. Jeya, and S. Petchiammal, "Accurate and Fast Iris Segmentation," International Journal of Engineering Science and Technology, vol. 2, pp. 1492-1499, 2010.

[5] H. A. Hashish, M. S. El-Azab, M. E. Fahmy and M. A. Mohamed, "A Mathematical Model for Verification of Iris Uniqueness," International Journal on Computer Science and Network Security, vol. 10, pp. 146-152, June 2010.

[6] Ales Muron, J. Pospisil, "The human iris structure and its usages," Acta Univ. PalackiOlomuc. Fac. Rerum Nat. Physica, vol. 39, pp. 87-95, 2000.

[7] R. P. Wildes, "Iris Recognition: An Emerging Biometric Technology," Proceeding of IEEE, vol. 85, no. 9, pp. 1348-1363, Sep. 1997

[8] S. Floyd, V. Jacobson. Random early detection gateways for congestion avoidance. IEEE/ACM Transactions on Networking (TON) August 19932309

[9] RFC: Recommendations on Queue Management and Congestion Avoidance in the Internet.

[10] A. Snoeren, C. Partridge, et. al., "Single Packet IP Traceback," IEEE/ACM Trans. Networking, vol. 10, pp. 721-734, Dec. 2002.

[11] E. R. Davies: Machine Vision. 3rd Edition: Elsevier (2005)

[12] Daugman J. (2001) Statistical richness of visual phase information: Update on recognizing persons by their iris patterns. International Journal of Computer Vision 45(1): 25-38.

[13] V. Chasanis, A. Likas, N. Galatsanos, "Simultaneous Detection of Abrupt Cuts and Dissolves in Video Using Suport Vector Machine". ELSEVIER Pattern Recognition Letters, No. 30, 55-65, 2009.

[14] S.Maheshwari, R. B. Pachori, and U. R. Acharya, "Automated Diagnosis of Glaucoma Using Empirical Wavelet Transform and Correntropy Features Extracted from Funds Images", IEEE Journal of Biomedical and Health Informatics, 2016.

[15] A. K. Al-Azzawi, M. I. Saripan, A. Jantan, R. W. Rahmat, A Review of Wave-net Identical Learning & Filling-in in a Decomposition Space of (JPG-JPEG) Sampled Images. Artificial Intelligence Review. 34(4), 309-342 (2010).

[16] Pedro F. Felzenszwalb and Ross B. Girshick and David McAllester and Deva Ramanan, "Object Detection with Discriminatively Trained Part-Based Models", IEEE Transactions on Pattern Analysis and Machine Intelligence, Vol. 32, pp. 1627- 1645, 2010.

[17] B. Leibe, A. Ettlin, B. Schiele. Learning Semantic Object Parts for Object Categorization, Image and Vision Computing, Vol. 26, No. 1, pp. 15-26, 2008.

[18] Ulrike von Luxburg; A tutorial on spectral clustering; Stat Comput (2007) 17: 395–416; DOI 10.1007/s11222-007-9033-z /Tubingen, Germany.